



Simulation of Diffraction and Reflections of arbitrary order with the Sound Particle Diffraction Model based on the Uncertainty Relation

Stefan Weigand, Alexander Pohl, Uwe Stephenson
Acoustics Group, HafenCity University, Hamburg, Germany.

Summary

In room and city acoustics, beside reflections, screening effects become important, often even of higher order. There are even cases where sound reaches immission points solely by diffraction. For these applications, ray tracing methods are appropriate and well established. These, however, are unable to simulate diffraction effects in a generally correct way. Standards for noise control engineering (as the VDI 2720) still propose the old detour model (Maekawa) which however is only valid for single diffraction, not at arbitrarily shaped obstacles and not in cascade. For reflections, still the combination with the mirror image source method is proposed which is highly inefficient for higher orders. Stephenson's energetic sound particle diffraction model is based on the uncertainty relation ('the closer the bypass distance to an edge the wider the distribution of the diffracted secondary sound particles'). It has been well validated meanwhile by comparison with Svensson's exact wave-theoretical secondary edge source model. In principle, it is capable to be efficiently applied for general cases of arbitrary reflection and diffraction orders. Meanwhile it has also been extended to 3D diffraction at edges of arbitrarily shaped apertures. In this paper, some more realistic cases of single and double diffraction are presented combined with geometric and diffuse reflections. The results of some numerical experiments are discussed. The new algorithm extends the spectrum of feasible cases of numerical noise immission prediction considerably.

1. INTRODUCTION

Motivation

In recent years, the EU has put on programs to map noise immissions in cities and action plans for improvements. In sound propagation, various physical effects are involved the focus of which is here on reflection, scattering and diffraction, especially on their combination. However, in spite of standards [1], there are (beside other unknown and varying conditions, e.g. ground impedances, sound powers, weather conditions etc.) still many uncertainties how to simulate them in detail. Computation times are often huge – mainly due to the application of the recursive and hence inefficient [3] Mirror image Source Method (MISM)[2]. Nevertheless, still enormous discrepancies occur. These are often caused by oversimplifications, unclear algorithms or differently handled truncation criteria.

Furthermore, due to the standards, for the computation of screening (diffraction) effects, usually

Maekawa's simple 'Detour Law' (MDL) [4] is applied, i.e.: "the transmission degree T (=intensity with obstacle /intensity in free field) is about inversely proportional to the detour of a ray around an obstacle" (see eq. 3). However, it is applied even for higher diffraction angles or double diffraction around thick or non-rectangular obstacles as buildings, where it is wrong and principally should not be applied [5][6] (the formula for this extension in [1] is only a rough approximation of limited validity).

Basic Examples For Ambiguities of the Detour Law

- for paths 'in parallel' it is suggested to add the energetic transmissions degrees of detour paths around each of the three edges of an (rectangular) obstacle (and to truncated the sum at 1, if exceeded); but what about arbitrarily shaped screens with more than three open sides or non-convex shape? How many paths should be taken into account?
- for obstacles 'in series' (Fig. 1.), it is unclear if paths lie 'in series' or 'in parallel' and, hence, whether transmission degrees add or multiply. This is, obviously highly contractive and dubious in several cases.

(c) European Acoustics Association

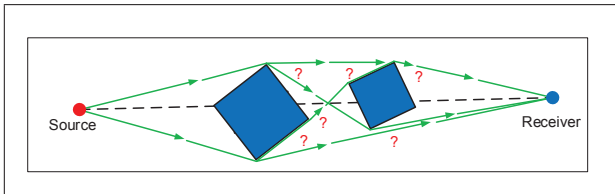


Figure 1. Some buildings 'in series' between source and receiver: Which of the transmission paths are relevant?

- c) in case of combination with reflections, it is tacitly assumed and praxis, to recursively mirror also diffracting edges (as with source points with the MISM), but the maximum reflection and diffraction orders to be taken into account are not defined (and can never be, in general);
- d) at higher reflection orders, most reflections are diffuse, but the MISM is not able to handle diffuse reflections, hence, they cannot be handled at all with these standard methods.

It is the main goal of this paper to show how this deficit can be overcome by use of the Sound Particle Simulation Method (SPSM) [7] in combination with the Uncertainty Relation based Diffraction Method (UBDM) [8], together called SPD (Sound Particle Diffraction). Cases of application in mind are room as well as city acoustics. However, room scattering as typically occurring and simulated for factory halls [14] is not yet considered here.

Basic hypotheses The typical room acoustics high frequency assumption of objects large compared with wavelengths, hence energetic superposition of sound particle energies, further: polygonal objects. Diffraction is mainly an edge effect. So, in this context, inspired by the Uncertainty-Relation (UR), the diffraction probability for sound particles (or angles) should be the stronger the closer the bypass distance to edges. So, in tracing particles, automatically, only 'important' edges have influence, the ineffective combination of all theoretically possible diffractions and reflections is avoided.

Both, the SPSM and the UBDM, have been extensively tested and validated in recent years, even for double diffraction and by part in 3D – however, not yet in more general, practical cases – examples of which shall be presented here. In simple cases (single diffraction and single reflection without scattering) the results can be compared with those of the detour model as a first reference – as shall be done here. In more general cases they have been validated with Svensson's exact wave theoretical Secondary Edge Source model (SESM)[10]. Both, the MDL and the SESM as deterministic models for given source-receiver-combinations, are destined to be combined with the MISM, so practically not able to combine diffractions with higher order reflections.

As usual for noise immission problems, here only the total sound levels are computed and mapped for an omni-directionally emitting point source.

2. SOUND IMMISSION PREDICTION METHODS- ALGORITHMS

In room and city acoustics, generally the numerical methods of geometric and statistic (i.e. energetic) room acoustics are applied. The MISM is a deterministic 'exact' model but indirect: it replaces reflecting surfaces by mirror image sources and then computes intensities directly by the $1/R^2$ -distance law. In contrast, with ray tracing (RT) methods, especially, as a sub-version, with the Sound Particle Simulation Method (SPSM), the $1/R^2$ -distance law is reproduced only statistically by counting sound particles (energy carriers) in 'detectors'. These are small volumes spatially extended around receiver points. It is an iterative Monte Carlo but straight forward method: nested loops over all particles, each all reflections, each testing all 'walls' for reflection [7]. A decisive advantage is: in contrast to the MISM, the SPSM is able to handle scattering effects.

In spite of this, the SPSM is (for a defined required level accuracy, at least in closed rooms with dominating reflections) much more effective than the MISM. With the MISM, the mirroring is a recursive process, the number of MIS and hence, the computation time, is exponentially growing with the reflection order. It can be shown [3] that the classical MISM is only efficient with low reflection orders (in many practical cases only 2-5). An efficient method to combine the advantages of straight forward RT with the exactness of the MISM is beam tracing (BT) that avoids most of the inefficient 'visibility tests.' BT works with receiver points and therefore is destined to be combined with diffraction simulation.

All these geometric methods naturally neglect diffraction.

2.1. Computing Sound levels and maps with the Sound Particle Simulation Method

While the tracing algorithm of SPSM is the same as with RT, the physical model behind is different. SPs carry single energies for all octave bands e_i instead of sound power in a flow of rays. The local sound energy density in a detector (volume V_d) is not only proportional to the number and energy of crossing SPs, but also on the time spend in the volume, hence, their crossing distances d_i . Based on this idea the sound particle detection formula [7] reads

$$I = \frac{P}{V_d \cdot M} \sum_{i=1}^N e_i \cdot d_i \quad (1)$$

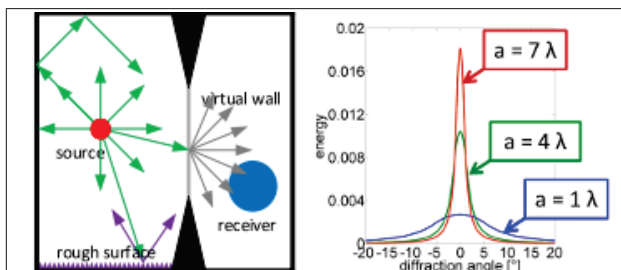


Figure 2. Principle of SPSM: Sound particles are emitted from the source evenly in every direction. They propagate on straight lines through the room until they hit a real or virtual wall. On hitting a real wall, specular (green arrows) and depending on the surface's scattering coefficient diffuse (purple arrows) reflections occurs. Virtual walls represent apertures, thus evoking diffraction (grey arrows). Finally sound particles pass a receiver where their energy is detected before they continue to propagate. Right: examples of DAPDFs.

where M is the number of SPs emitted, N of those having crossed and P is the fictive sound power of the source. The result is not dependent on the shape of the detectors, there is no directivity. So, also a grid of cubic detectors is allowed, which allows very efficient algorithms for detection – important for computing noise maps.

2.2. Models to compute reflection and scattering at surfaces

Geometric (specular) reflection is computed by mirroring the directional vector of a SP at the plane of the encountered wall. Absorption is factored in simply by multiplying the SPs energies with $(1 - \alpha)$, α being the usually frequency dependent but angle independent (diffuse field) absorption degree given for all octave bands from 125Hz to 8kHz.

Scattering from 'rough' walls ('rough' in depth of a profile compared to the wavelength) is a highly frequency and angle dependent wave effect. In room acoustical simulation, however, it is usually roughly simulated by an interpolation between geometric and 'totally' diffuse reflection, i.e. according to Lambert law:

$$\frac{dp}{d\Omega} = \frac{\cos(\theta)}{\pi} \quad (2)$$

(the reflected energy fraction or probability per solid angle is proportional to the cosine of the polar angle.) The 'roughness' is described by a scattering coefficient s (if 1, totally diffuse, if 0 specular). It is defined in ISO 17497-1 [11], as the ratio of the non-specular reflected sound energy E_{nspc} to the totally reflected energy E_{tot} (see Fig. 3).

This is directly simulated by splitting up an incident SP in two secondary SPs on hitting a wall. One is carrying the specular (partially absorbed, frequency

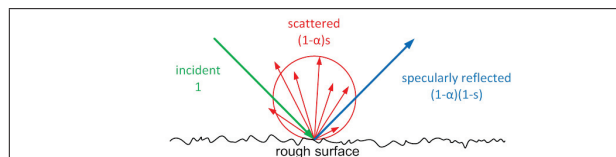


Figure 3. Visualisation of definition of scattering coefficient s and scattering due to surface roughness as modelled in the SPSM: Each sound particle hitting a rough surface is split up into 2 secondary sound particles. The first carrying specular energy, the second carrying the scattered energy in one randomly chosen direction according to Lambert law.

dependent) energies $(1 - s)(1 - \alpha)$ the other SP carries the scattered energy $s(1 - \alpha)$. Its direction is chosen randomly according to Lambert law.

It should be noted, that scattering is also caused already by the finiteness of a surface (the 'edge effect'. i.e. edge diffraction), this can be factored in by a summing up of both effects. This has not been done here. Instead, in case of 'scattering surfaces', realistic scattering coefficients have been used [13].

3. MODELS TO COMPUTE DIFFRACTION

3.1. Conventional approaches based on Kirchhoff

The old Kirchhoff approach is based on the assumption that the sound field behind a barrier can be computed by a (Helmholtz) surface integral over Huygens point sources on the 'aperture' around the obstacle and that it is undisturbed on the incident side and independent from flanking surfaces. These assumptions fit well to the energetic straight forward models of GSRA and are therefore common in engineering. For the important special case of just one barrier (a half-infinite screen), Fresnel's theory is valid [5]. For small diffraction angles, the transmission degree of the single screen is then about inversely proportional to the detour of a ray around the edge of the screen related to the wavelength- Maekawa's 'detour law':

$$T_{screen} \approx \frac{1}{3 + 20N} \quad (3)$$

where $N = z/(\lambda/2)$ is the Fresnel number and $z = a_Q + a_A - s_m$ (Fig. 4) the detour (the corresponding level correction in [1] is then $D_z = -10lg(T)$). A factor $C_2 = 10$ instead of the '20' in eq. 3 is specified to account for the doubling of energy by ground reflection. In case of double diffraction around the two edges of a building of width e (see Fig. figExpSetUpDouble), an empiric factor C_3 is introduced to multiply C_2 :

$$C_3 = \frac{(1 + (M/10)^2)}{(1 + (M/10)^2/3)}; \quad M := e/(\lambda/2) \quad (4)$$

The classical complementary case is the slit of width $b[\lambda]$. For parallel incidence, also receivers in far field, and small angles ε , the diffraction pattern is the Fourier transform of the transfer function of a slit, the famous slit function $T_{slit} \propto (\sin(u)/u)^2$ with $u = \pi b\varepsilon$.

3.2. Exact wave theoretical models

Based on the exact solution for the diffraction at an infinite wedge by Biot, Tolstoy and Medwin, Svensson [10] developed the 'Secondary Edge Source Model' (SESM) allowing also finite edges. The SESM assumes that the total sound pressure is superimposed by the direct and specular reflected and, as a correction, the diffracted sound field made up by the radiation from the edges (computed by integration). Different from the UBDM, the boundary conditions of the hard flanking walls of a wedge are taken into account. The SESM is destined to be combined with the MISM. The Geometrical Theory of Diffraction, improved with the Uniform Theory of Diffraction (UTD, [15]), is a high-frequency asymptotic solution which has been developed to be applied to ray tracing of radar waves, it has already been combined with acoustical beam tracing. However, this method is made only for small frequency bands. Concerning combination with RT, the problem of all these 'exact' methods is: rays never hit edges exactly; they pass only near-by. This has been the point to introduce the UBDM.

3.3. The Uncertainty Relation based Diffraction Method (UBDM)

To repeat the UBDM in short: There are two basic concepts of implementation of the uncertainty relation (UR) ('the closer a SP passes edges the more it is deflected'): the Diffraction Angle Probability Density Function (DAPDF) and the Edge Diffraction Strength (EDS) [8].

The SP should behave as if it 'sees' an imaginary slit of a width b proportional to the bypass distance a (in units of λ , it turned out that $b = 6a$). Therefore, the DAPDF (see fig.4, to the right) is derived from the Fraunhofer diffraction at a slit (see 3.1.) simplified by averaging over a wide frequency band, the simplest but still well working formula is:

$$D(v) = D_0 / (1 + 2v^2), \quad \text{with } v = 2b\varepsilon \quad (5)$$

where ε is the deflection angle and D_0 is a normalization factor.

To develop a modular model which is applicable also to several edges that are passed near-by simultaneously (distances a_i), the notion of an 'Edge Diffraction Strength' ($EDS(a)$) is introduced such that the EDS of several edges may be added up to a total $TEDS$:

$$TEDS = \sum EDS_i = \sum \frac{1}{6a_i} =: \frac{1}{b_{eff}} \quad (6)$$

with the 'effective slit width' b_{eff} .

Implementation: To detect diffraction events, it is necessary to introduce so called virtual walls as apertures 'above' all 'inner' edges. It turned out that most practical for that is a subdivision of the room into convex subspaces. When a sound particle hits a virtual wall it is split up into S evenly distributed secondary sound particles. Each secondary SP's energy is partitioned according small angular integrals over the DAPDF. The bypass distances a_i are measured on these virtual walls. To ensure reciprocity [9], however, the shortest bypass distances are found to be relevant which are, with incident angles ε_1 : $a'_1 = a_1 \cos(\varepsilon_1)$.

Recently, the UBDM has been extended to 3D [9]. Basic idea is: The UR is valid independently in 2 orthogonal directions, here according a local coordinate system of a polygonal aperture. The respective 2D-DAPDFs multiply. Hence, there are four DAPDF input parameters: two diffraction angles, ε and η and two effective slit widths b_1, b_2 computed each from two bypass distances to opposite sides computed from summing up their EDS s.

A practical problem is: the necessary integration of the resulting 3D-DAPDF over the small solid angles of each SP is analytically not possible and numerically time consuming. This is not acceptable for each diffraction event. Hence, results for all SP energy fractions have been calculated once in advance in a 4-dimensional matrix (database) and are interpolated at runtime [17].

4. NUMERICAL EXPERIMENTS

For this paper three scenarios are examined. First, a simple single-barrier scenario is used to examine the influence of a wall behind the barrier with different acoustic properties (test surface). Then a double barrier scenario with different floor or roof materials in between the barriers (test surface) is being evaluated, respectively. Last, a building with slightly scattering walls standing on a scattering floor is simulated as a realistic scenario.

For evaluating the effects of a combination of diffraction and scattering three levels of physical modelling are compared: a model only applying diffraction (Diff), one applying diffraction and specular reflections (Spec) and finally a model applying diffraction and specular as well as diffuse reflections (Scatt). The first is simulated using an full absorbent test surface (III in Fig. 4), the former two are compared using the same surface properties of a typical scatterer ($s = \{0.06, 0.35, 0.57\}$, $\alpha = \{0.015, 0.025, 0.06\}$ for the frequencies shown here), enabling or disabling scattering in the simulation.

Moreover results according to [1] including mirror image sources and diffraction of first order are calculated for designated receiver positions R_i .

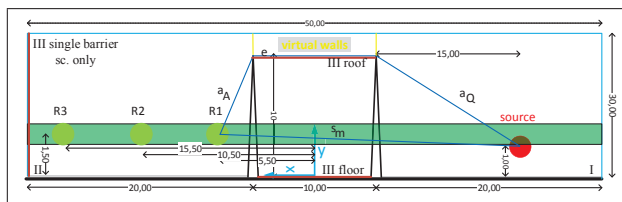


Figure 4. Sketch (not to scale) of double-barrier scenario (side view). Dimensions in meters. Designated receiver points are marked with green circles, labelled $R_1 \dots 3$. Evaluation line is marked by a green bar. Single barrier scenario is similar, just without the distance in between the two barriers and the reflecting wall on the very left instead of the reflecting floor.

4.1. General Experimental Set-Up

The set-up is depicted in Fig. 4 for the double barrier scenario, single barrier is similar. An omnidirectional source emitting 50.000 primary sound particles equally is used. The source power is 1 W in the range of 125 Hz to 8 kHz. A grid receiver is employed, made up of cubic voxels with length 1 m, unless noted otherwise. Receiver grid spans the whole simulation region. Diffraction is simulated with $S = 2.000$ secondary sound particles. Energetic abortion criterion is 10^{-12} of the source power.

The models' bounding box ($L \times W \times H$: 50 m \times 40 m \times 30 m) is full absorbent, yielding free-field conditions. The barrier (10 m high) is positioned at $x = 0$ (single) and $x = \pm 5$ m (double), spanning the whole simulation region's width. The source is positioned at 15 m in front of the barrier, 1 m above ground. It is full absorbent.

The ray like patterns in the upper left corner (view zone) at high frequencies are due to undersampling occurring at this combination of detector size and sound particle number. However this region is of minor interest (Fig. 5-7).

4.2. Single Barrier Scenario

The floor is full absorbent. The surface of the wall behind the barrier is varied as described before.

Evaluation is done in the plane given by $z = 0$. Fig. 5 shows nine noise maps (colour coded sound intensity levels in dB). It is organized in rows and columns: rows representing different frequencies, columns representing Diff, Spec and Scatt.

The effects of diffuse reflections combined with diffraction can be seen by comparing noise maps 5 and 6 in Fig. 5: While Spec brings only little energy in the region behind the barrier, Scatt 'enlightens' even the deep shadow zone. For high frequencies (noise maps 8 vs. 9) the influence of scattering becomes even more important, as the region behind the barrier is not served by diffraction any more. However the diffuse other than the specular reflecting back wall brings energy to this region. For low frequencies the influence

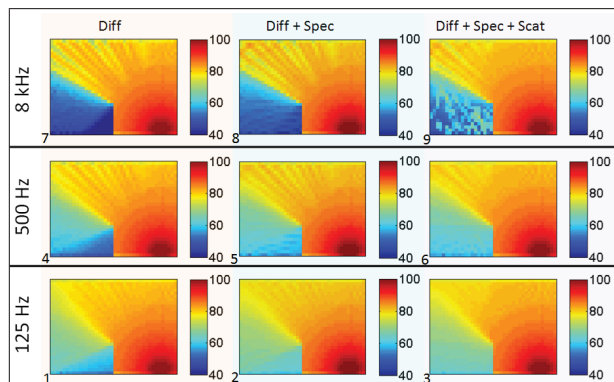


Figure 5. Results of single barrier scenario. Colour coded sound intensity levels in the $z = 0$ plane. Range: 40 dB to 100 dB.

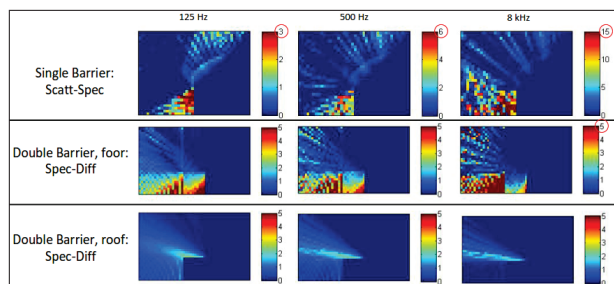


Figure 6. Sound intensity level difference plots. Single wedge colour map is between 0...3/6/15 dB, double wedge colour maps between 0...5 dB (larger values binned to max value). No difference plots Scatt-Spec are shown for double wedge scenarios, as no significant differences occurred here (less than 0.5 dB).

of scattering is small, as expected since the scattering coefficient is small, too.

For a better quantitative evaluation the upper row of Fig. 6 shows the difference Scatt-Spec. Mind the different scales! For low frequencies the gain due to scattering is up to 2 dB. For medium frequencies it's in the range of 3...5 dB. For high frequencies it is around 10 dB, reaching up to 20 dB.

4.3. Double Barrier Scenario

In the double barrier scenario, the barriers are positioned at $x = \pm 5$ m. Barriers are absorbent, as well as the floors I and II (s. Fig.4). The source is as described before. The floor between the barriers is varied as described earlier, yielding Diff, Spec and Scatt.

Again, evaluation was done for $z = 0$. Fig. 7 shows noise maps for double wedge floor and roof scenario, respectively. Obviously, there is hardly any difference between the roof and floor scenario. It could be shown that there is virtually no difference whether the floor was specular or diffusely reflecting (no figure), too. However comparing Diff with Spec it shows that regarding reflections in between barriers is important.

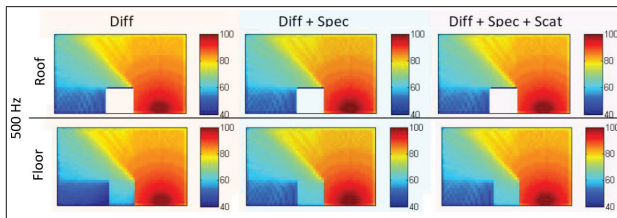


Figure 7. Results for double barrier scenario, with roof and floor as test surface at 500 Hz. Colour coded sound intensity levels in the $z = 0$ plane. Range 40 dB to 100 dB.

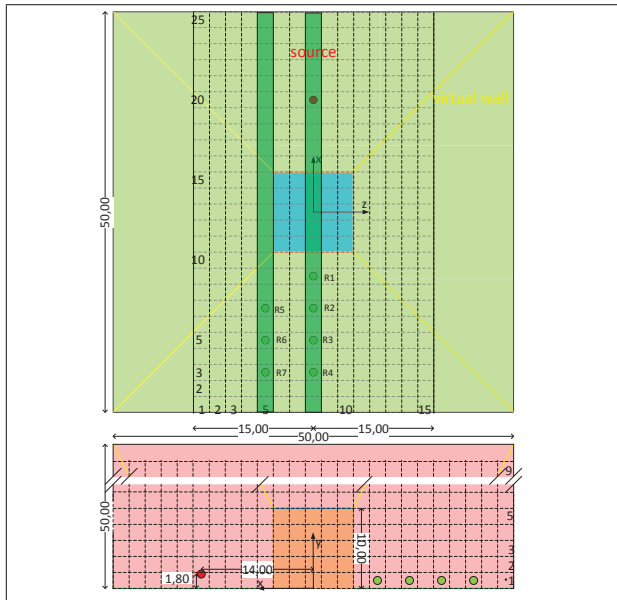


Figure 8. Scaled sketch of geometric set-up for the 'building on brushed stone'-scenario: Dimensions are in meters, receiver grid ($2 \times 2m^2$) is given with indices for each voxel. Source is at $S(14, 1.8, 0)$.

4.4. Cubic Building on scattering floor

The last scenario aims at modelling a typical 3D situation with a realistic building: a cubic building with brick walls and concrete rooftop on a scattering floor (debris, brushed stones, average size 10 cm, 40% coverage). Absorption coefficients were taken from the PTB database [12], scattering coefficients were calculated or interpolated according to [13]. A scaled sketch of the building along with source, receiver grid and designated receivers is depicted in Fig.8. Results for this scenario will be presented during the congress.

5. CONCLUSIONS AND OUTLOOK

It could be shown that considering diffuse reflections within barrier scenarios can be important. Detour methods fail here. Moreover reflections between barriers are important, also for the space behind the second barrier. Further numerical experiments with 3D sound particle diffraction are planned.

Due to the recursive split-up of sound particles at higher order diffraction, the computation time ex-

plodes. This has to be overcome by a re-unification of sound particle energies. This is achieved [by discretising the room surface into many patches and collecting energy on them as with the radiosity method,] for arbitrary combinations of diffuse or specular reflections with diffractions, by the Sound Particle Radiosity Method (SPRAD), which already has been implemented [18].

References

- [1] ISO 9613: Acoustics - Attenuation of sound during propagation outdoors, 1996
- [2] Borish, J.: Extension of the image model to arbitrary polyhedra. *J. Ac. Soc. Am.* 75 (1984), p. 1827-1836
- [3] Stephenson U.,M.: Comparison of the Mirror Image Source Method and the Sound Particle Simulation Method, *Applied Acoustics* 20 (1990), H1, p.35-72
- [4] Maekawa, Z.: Noise reduction by screens, *Applied Acoustics* 1 (1968), p.157-173
- [5] Pierce, A.D.: Diffraction of Sound around corners and over wide barriers. *J. Ac. Soc. Am.*, 55 (1974).
- [6] Kurze, U.J.: Noise reduction by barriers, *The Journal of the Acoustical Society of America* 55:504-518, (1974)
- [7] Stephenson, U.: The Sound Particle Simulation Technique - An Efficient Prediction Method for Room Acoustical Parameters of Concert Halls, Repr. 86th AES Convention, Hamburg (1989)
- [8] Stephenson, U.M.: An Energetic Approach for the Simulation of Diffraction within ray Tracing based on the Uncertainty Relation, *ACUSTICA united with acta acustica*, 96 (3) (2010) p. 516-535
- [9] A. Pohl: Simulation of Diffraction Based on the Uncertainty Relation, PhD thesis, HCU Hamburg, 2014
- [10] U. P. Svensson, R. I. Fred, and J. Vanderkooy, An analytic secondary source model of edge diffraction impulse responses, *The Journal of the Acoustical Society of America* 106 (1999), p. 2331-2344
- [11] ISO/FDIS 17497-1: Acoustics - Measurement of the sound scattering properties of surfaces - Part 1, 2004
- [12] Physikalisch Technische Bundesanstalt: Materialdatenbank, Braunschweig,
- [13] J.H. Rindel: Room Acoustic Prediction Modelling. In *Proc. Encontro SOBRAC*, Salvador, Brazil, 2010
- [14] Stephenson, U.M.: A Sound Particle Scattering Model Simulating Sound Propagation in Factory Halls; In: *Proc. INTERNOISE*, Göteborg (Sweden), 1990, p. 243-246
- [15] Kouyoumjian, R.G., Pathak, P.H.: A Uniform Geometrical Theory of Diffraction for an Edge in a Perfectly Conducting Surface. *Proc. of the IEEE*, 1974, p. 1448-1461
- [16] A. Pohl, U. Stephenson: Efficient simulation of sound propagation including multiple diffractions in urban geometries by convex sub-division. In *Proc. of Inter-noise*, Lisbon, Portugal, 2010
- [17] S. Weigand, A. Pohl, U. Stephenson: Bestimmung des Einflusses der Parameter-Unsicherheiten innerhalb des Schallteilchen-Beugungs-Verfahrens, In *Proc. of DAGA*, Nürnberg, Germany, 2015
- [18] Pohl, A. and Stephenson, U.M. A combination of the sound particle simulation method and the radiosity method, *Building Acoustics* (New Zealand), 2011